Electronic Supplementary Information

Cobalt Nanoparticles Incorporated into Hollow Doped Porous Carbon Capsules as Highly Efficient Oxygen Reduction Electrocatalyst

Feng Guo,*[ab] Hui Yang,*[b] Briana Aguila,[b] Abdullah M. Al-Enizi,[c] Ayman Nafady,[cd] Mandeep Singh[e], Vipul Bansal[e] and Shengqian Ma *[bc]

[a]School of Chemistry and Chemical Engineering, Yangtze Normal University, 16 Juxian Rd, Fuling, ChongQing, 408100 China.

Email: *guofeng1510@163.com*

[b]Department of Chemistry, University of South Florida, CHE205A, 4202 E. Fowler Avenue, Tampa, Florida, 33620, U.S.A.

Email: *huiy@mail.usf.edu; sqma@usf.edu*

[c]Chemistry Department, College of Science, King Saud University, Riyadh, 11451, Saudi Arabia

[d]Chemistry Department, Faculty of Science, Sohag, 82524, Egypt

[e]Ian Potter NanoBioSensing Facility, NanoBiotechnology Research Laboratory, School of Science, RMIT University, Melbourne, VIC, 3000, Australia

Electrochemical related calculations

All the current density in this work was calculated based on the geometrical area of rotating disk electrode. The numbers of electrons transferred (n) during ORR was calculated by Koutecky–Levich equation, at various electrode potentials:

$$1/j = 1/j_L + 1/j_K = 1/B\omega^{1/2} + 1/j_K \quad \text{(i)}$$

$$B = 0.62nFC_0D_0^{2/3}v^{-1/6} \quad \text{(ii)}$$

$$j_K = nFkC_0 \quad \text{(iii)}$$

where j is the measured current density; j_K and j_L are the kinetic and diffusion−limiting current densities, respectively; ω is the angular velocity of the disk (= 2πN, N is the linear rotation speed); n represents the overall number of electrons transferred in oxygen reduction; F is the Faraday constant (F = 96485 C mol^{-1}); C_0 is the bulk concentration of O_2 (1.2×10^{-6} mol cm^{-3}); D_0 is the diffusion coefficient of O_2 in 0.1 M KOH electrolyte (1.9×10^{-5} cm^2s^{-1}); v is the kinematics viscosity for electrolyte, and k is the electron−transferred rate constant.

For RRDE tests, the disk electrode was scanned catholically at a rate of 5 mV s^{-1} and the ring electrode potential was set to 1.30 V vs. RHE. The hydrogen peroxide yield (H_2O_2 wt%) and the electron transfer number (n) were determined by the following equations:

$$H_2O_2\ (wt\%) = 200*(N_r/N)/(I_d+I_r/N)$$

$$n = 4*(I_d)/(I_d+I_r/N)$$

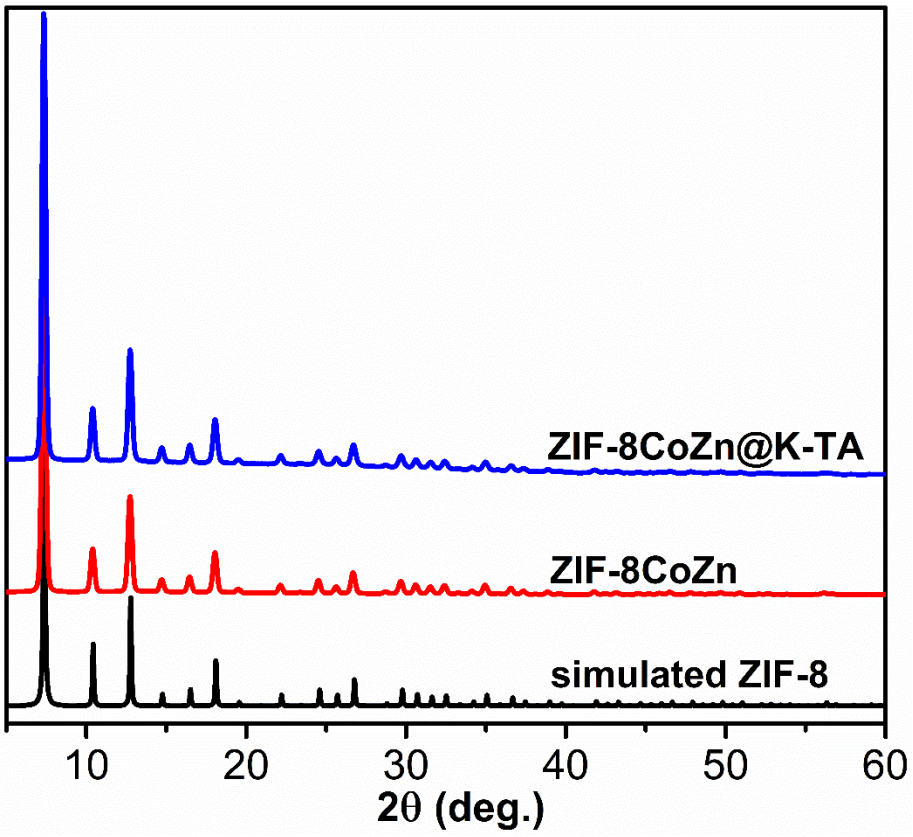

Fig. S1. PXRD patterns of materials.

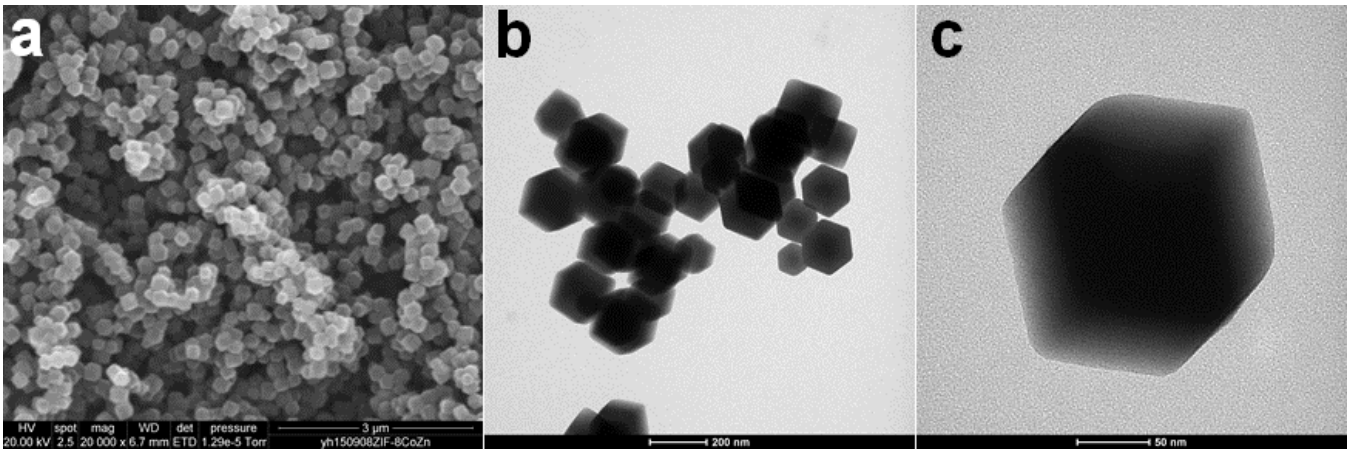

Fig. S2. SEM and TEM images of ZIF-8CoZn.

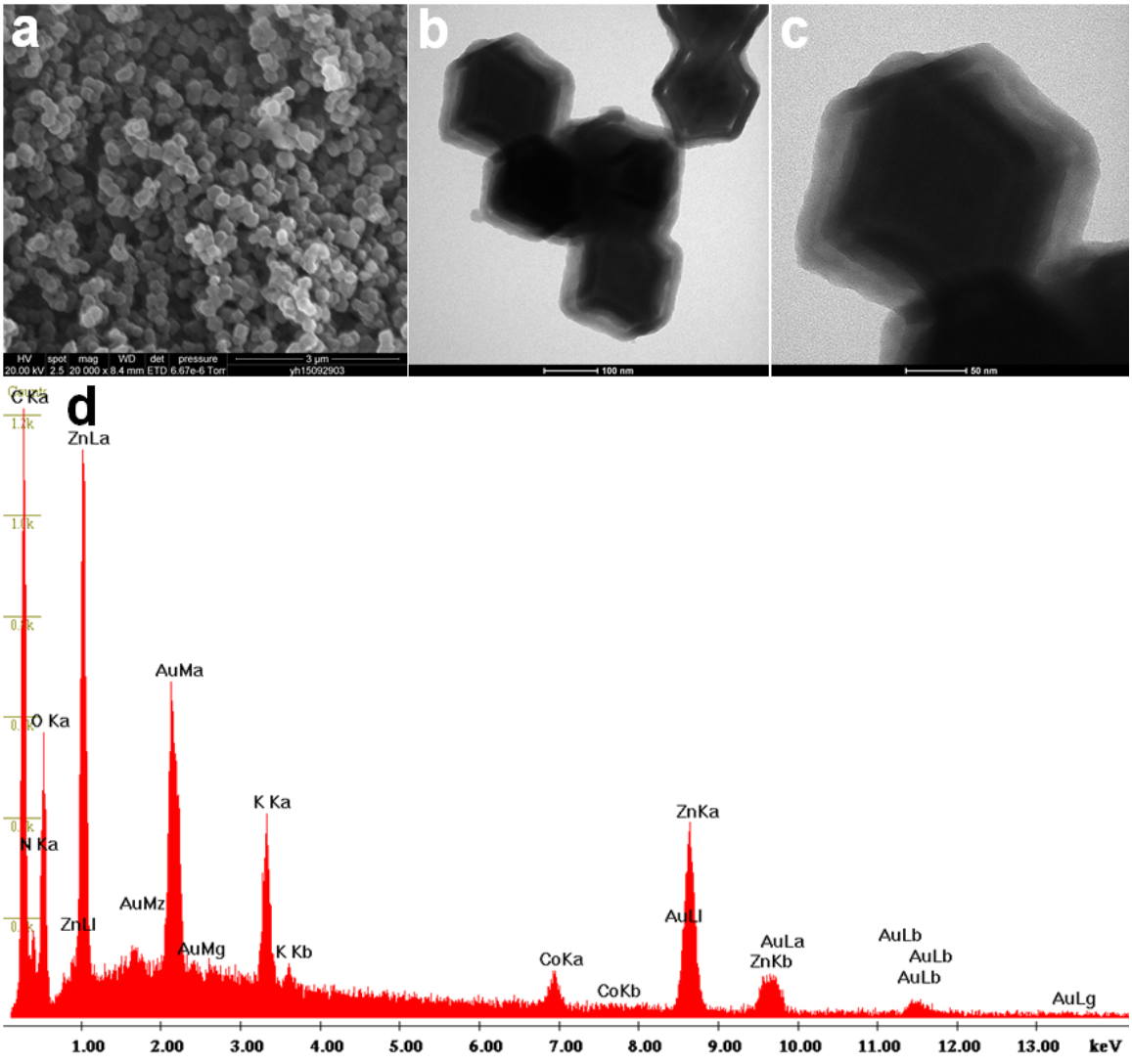

Fig. S3. SEM, TEM images and EDS spectrum of ZIF-8CoZn@K-TA.

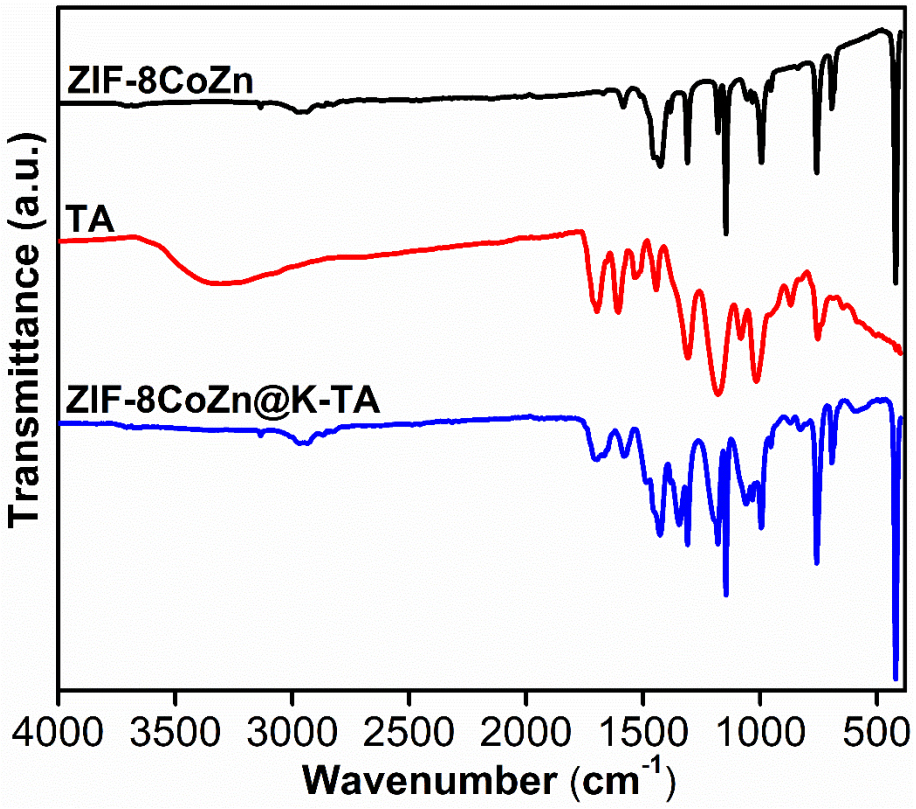

Fig. S4. FTIR spectra of each material.

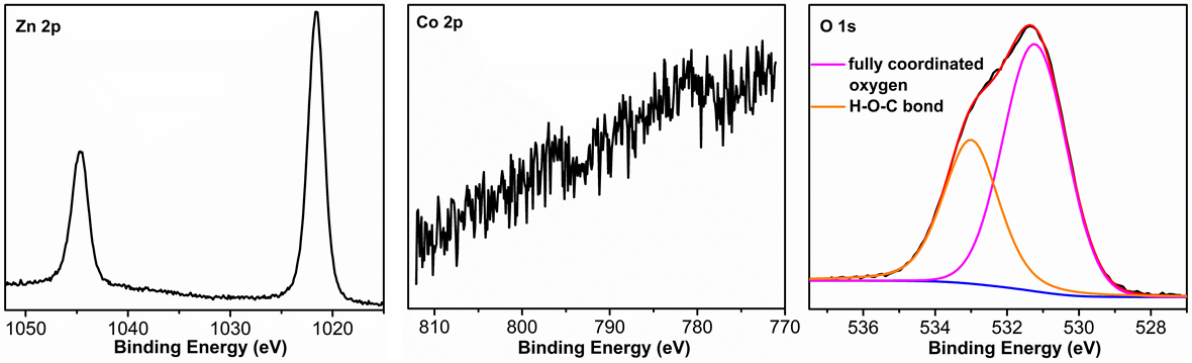

Fig. S5. Zn 2p, Co 2p, and O 1s XPS spectra of ZIF-8CoZn@K-TA.

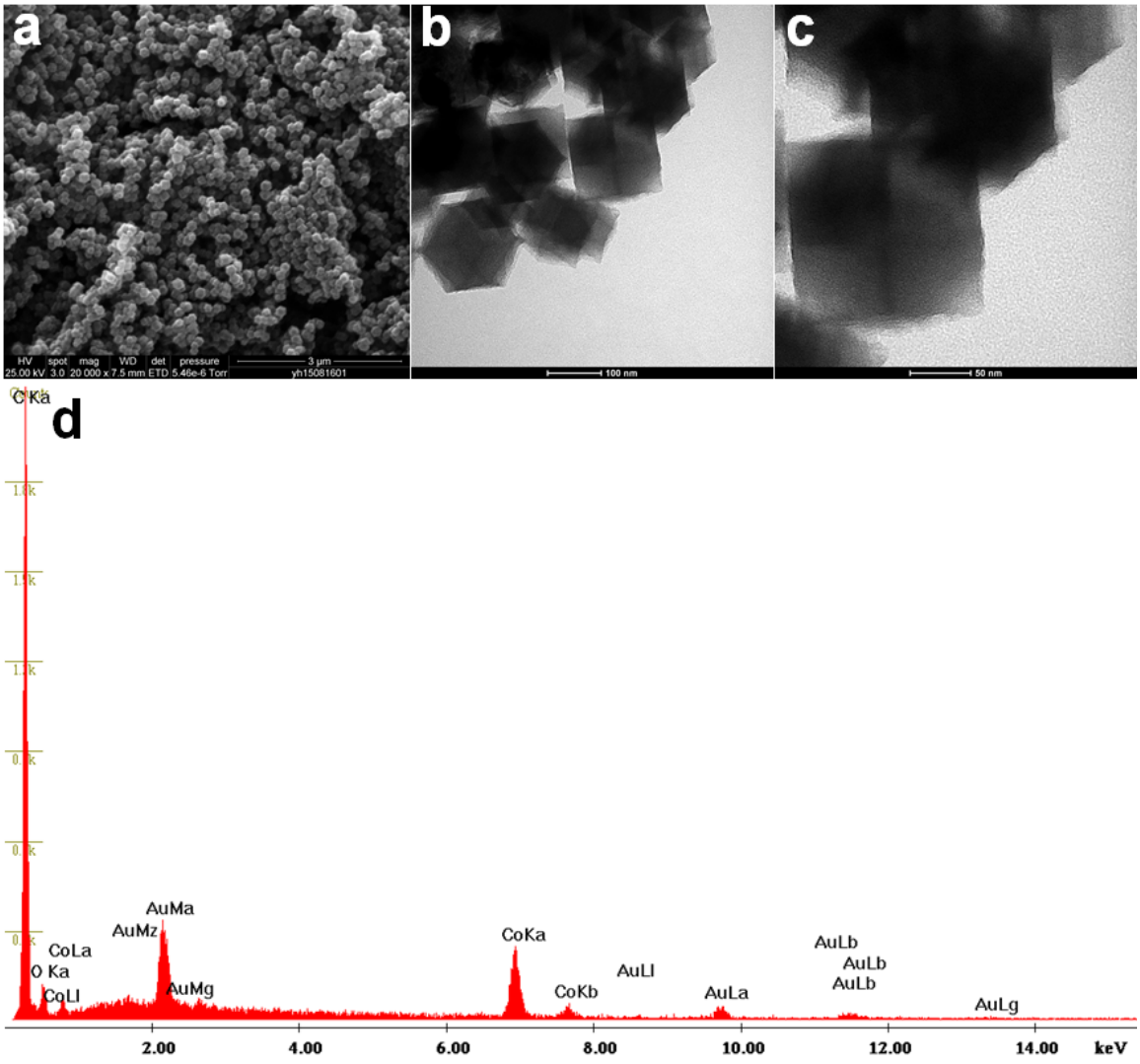

Fig. S6. SEM, TEM images and EDS spectrum of Co/NC.

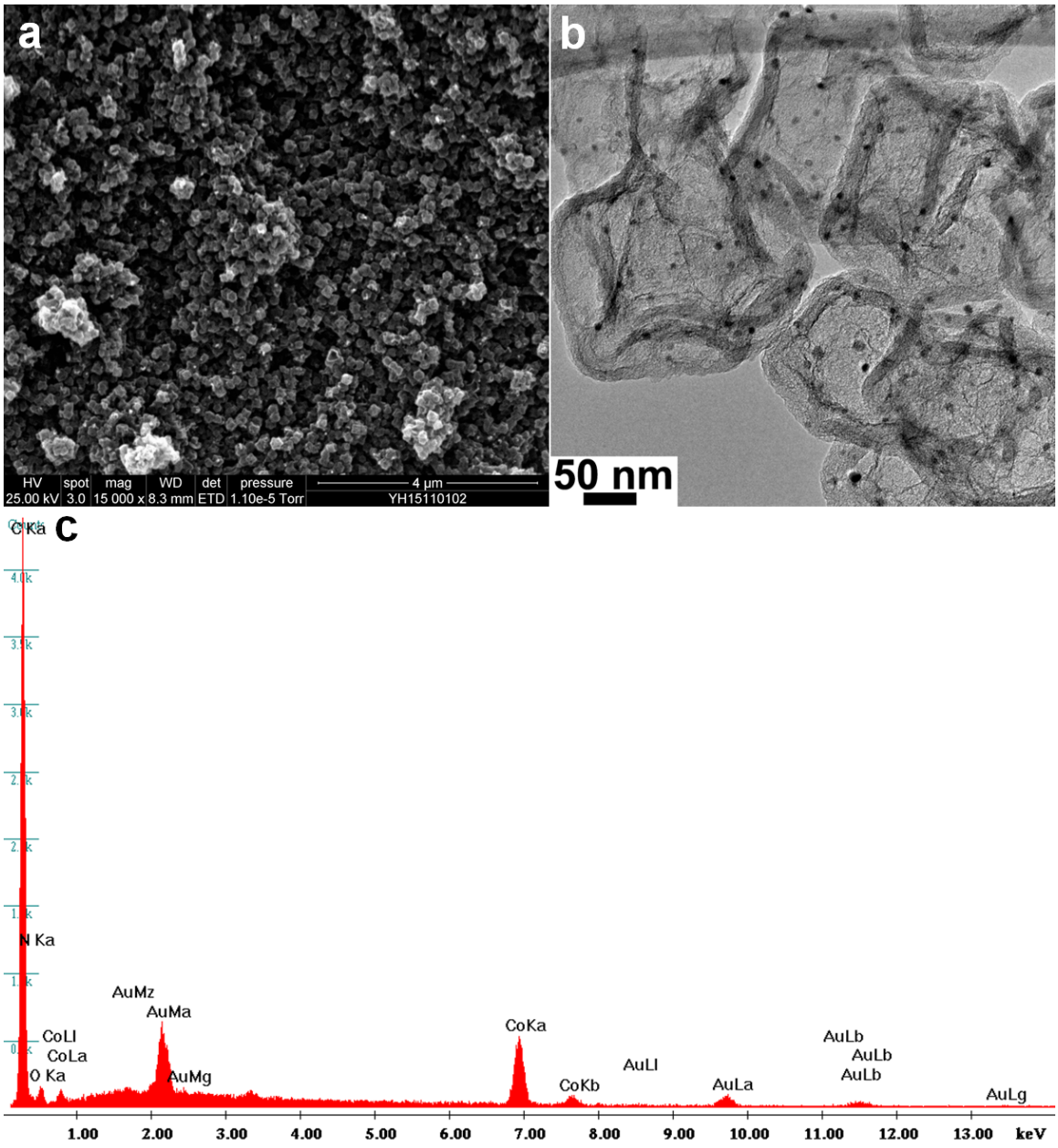

Fig. S7. SEM, TEM images and EDS spectrum of Co@NPCC.

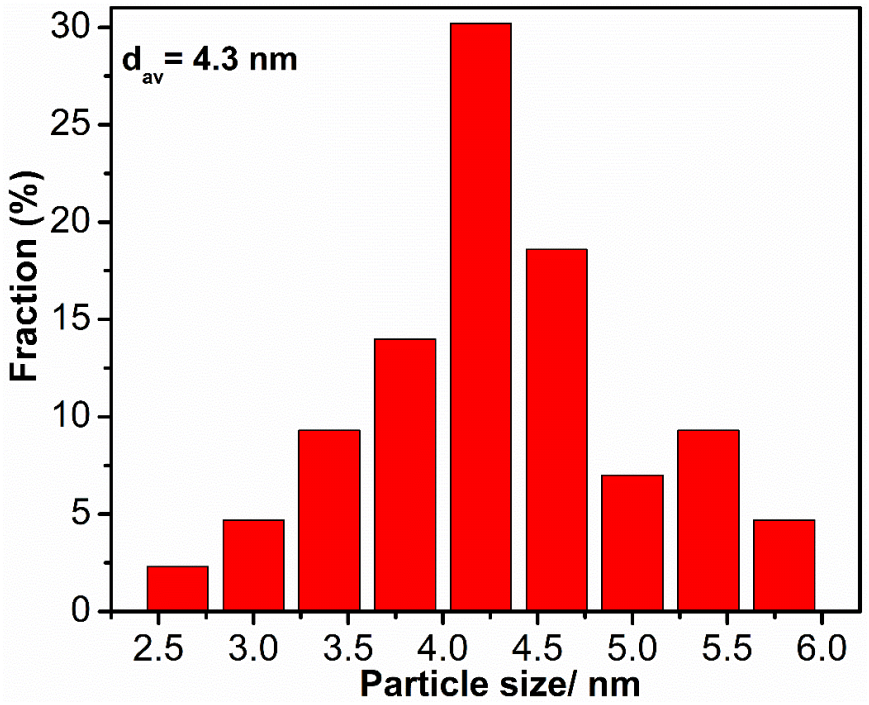

Fig. S8. Histogram of nanoparticle and average particle size for Co@NPCC.

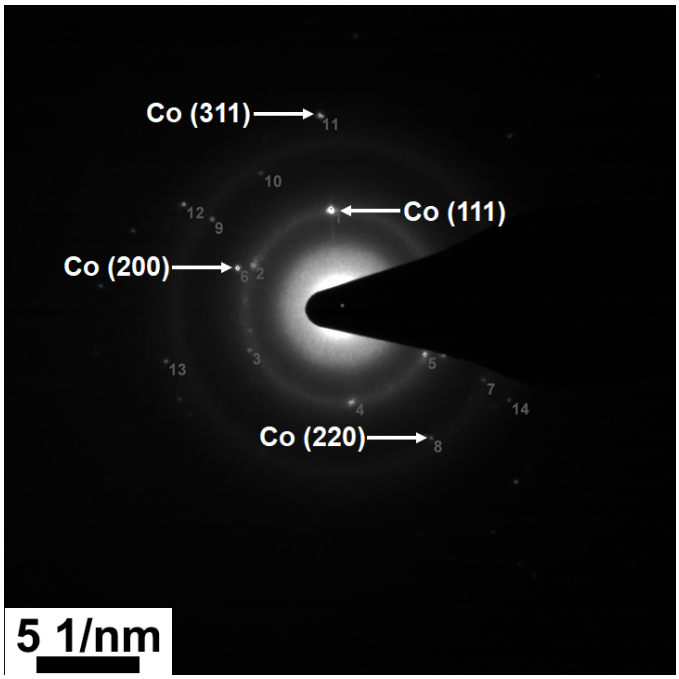

Fig. S9. SAED pattern of Co@NPCC

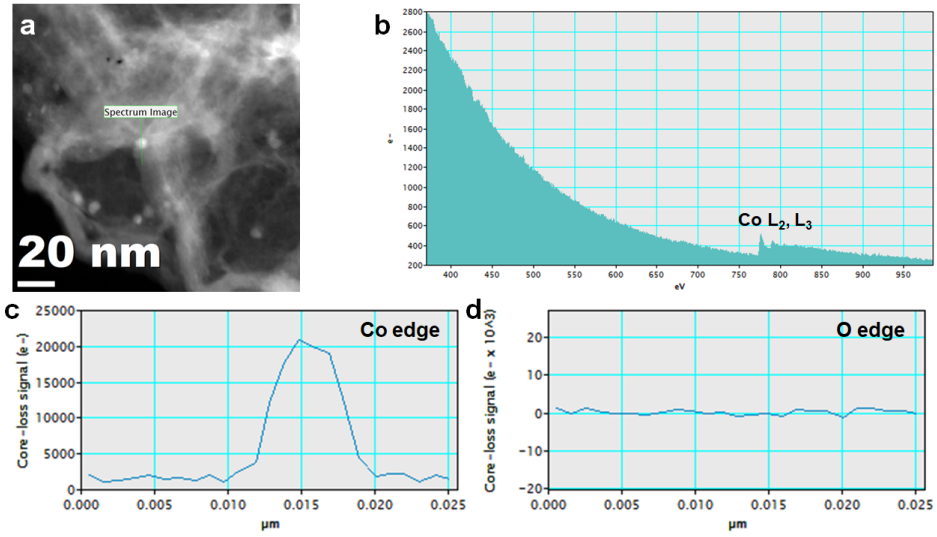

Fig. S10. HAADF-STEM image (a) with accompanying EEL point spectrum (b). The point spectrum in (b) was taken on the bright atom in (a). Co-edge (c) and O-edge (d) line profiles along the line on a.

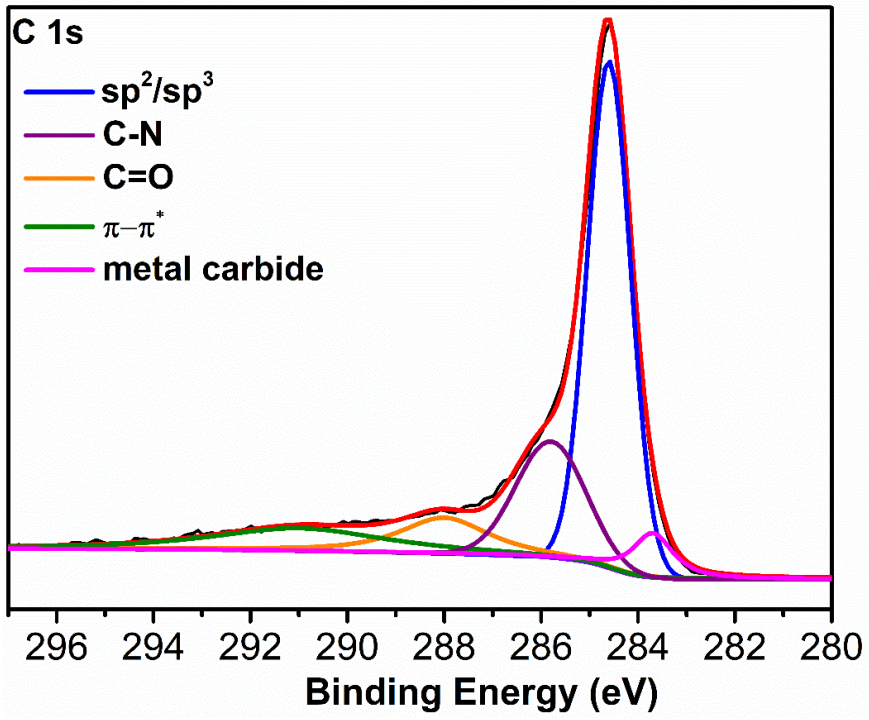

Fig. S11. C 1s XPS spectrum of Co@NPCC.

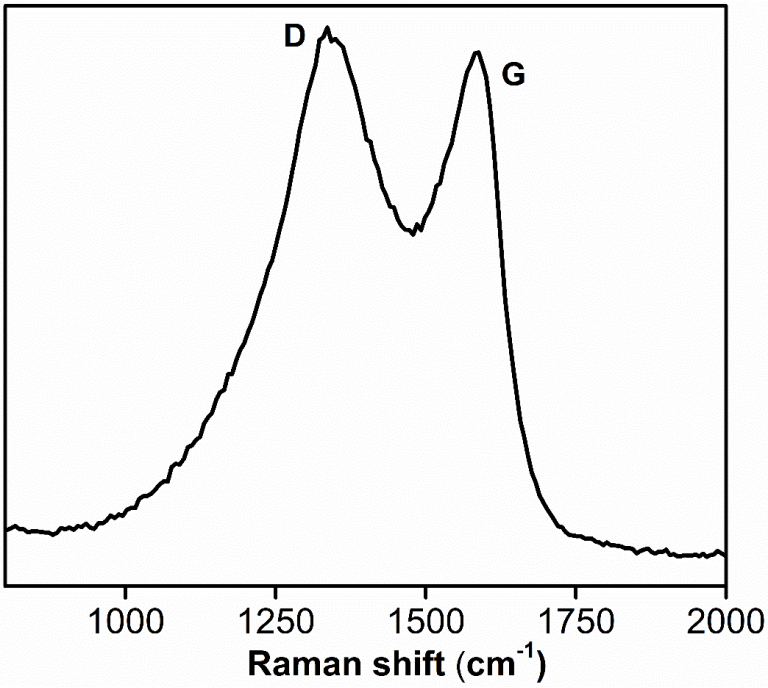

Fig. S12. Raman spectrum of Co@NPCC.

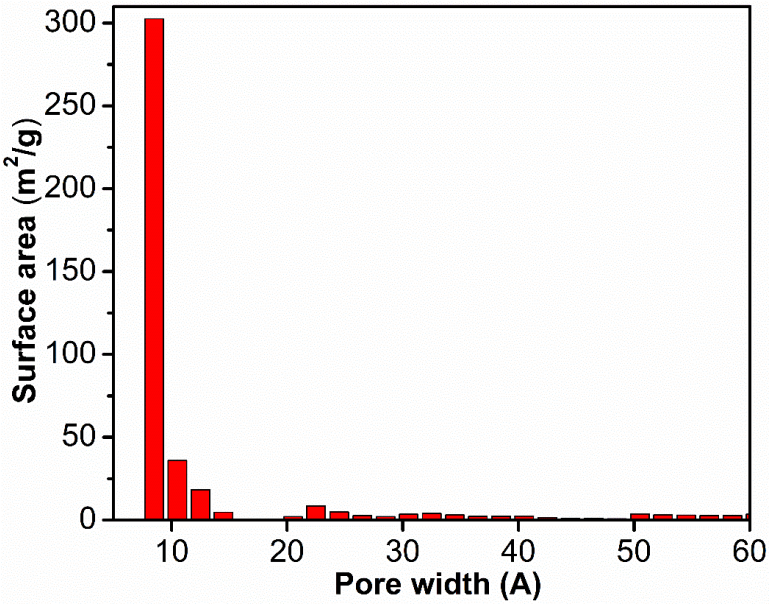

Fig. S13. Pore size distribution plot of Co@NPCC calculated using a DFT method from N_2 isotherms measured at 77 K.

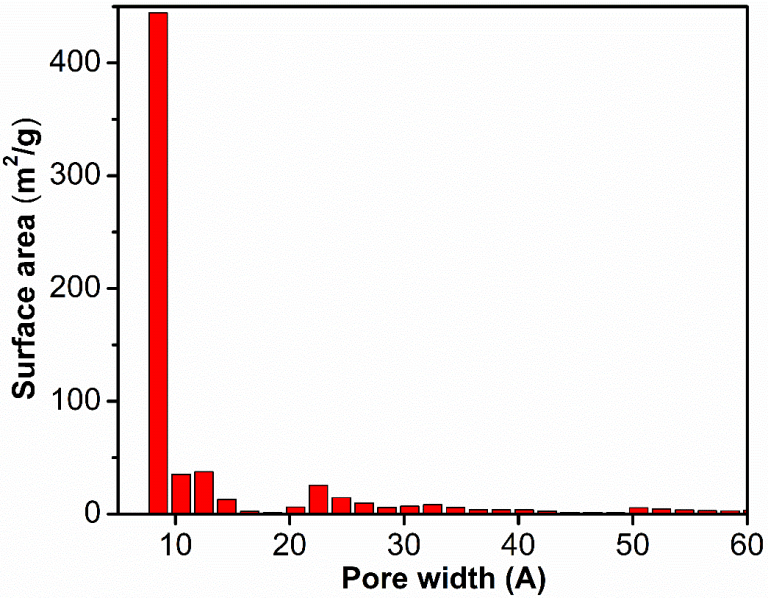

Fig. S14. Pore size distribution plot of Co/NC calculated using a DFT method from N_2 isotherms measured at 77 K.

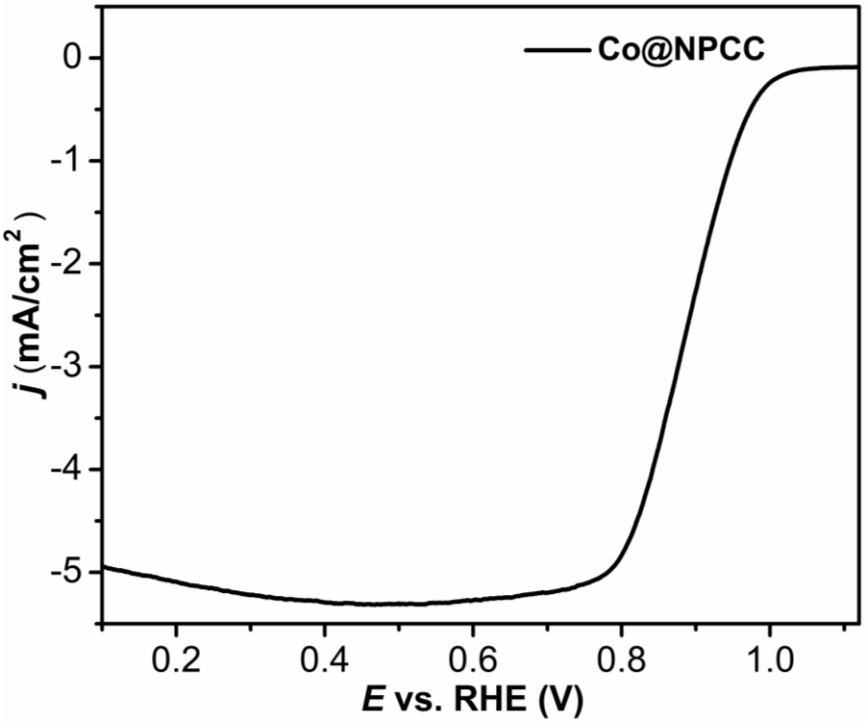

Fig. S15. LSV cure of Co@NPCC in 0.1 M KOH by RRDE technique.

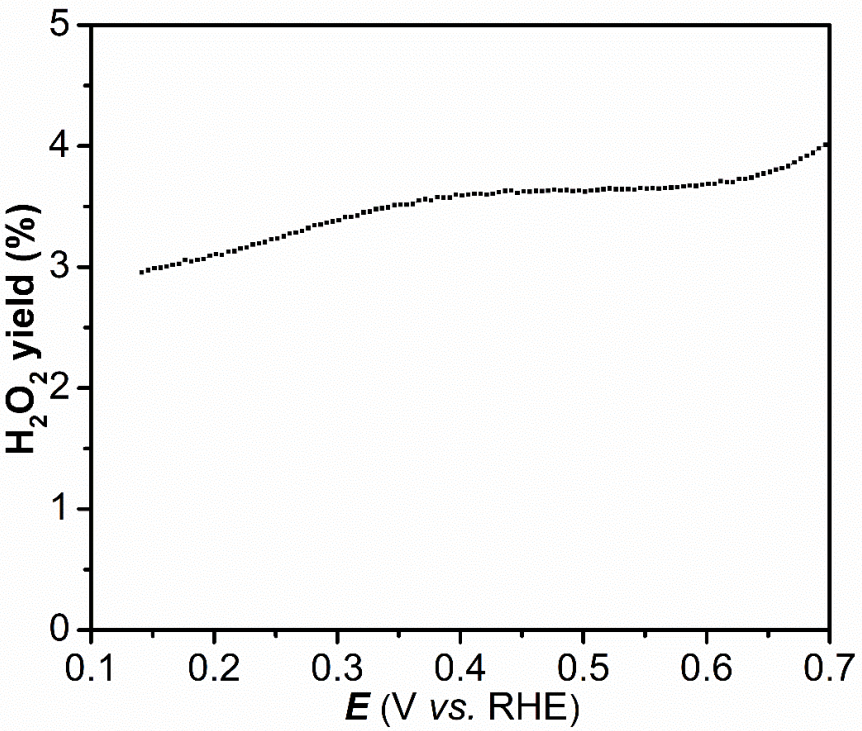

Fig. S16. H_2O_2 yield of Co@NPCC in 0.1 M KOH.

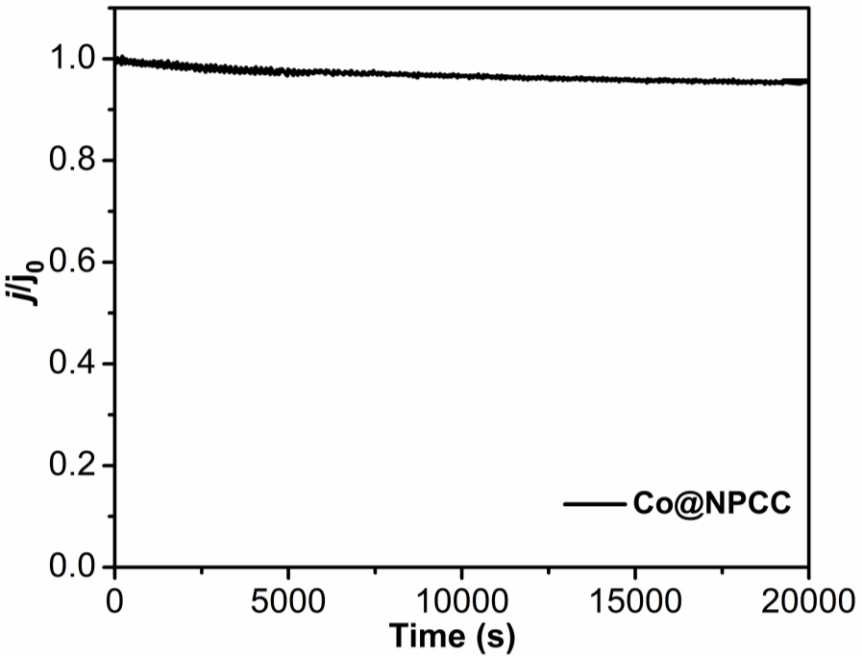

Fig. S17. The chronoamperometric test of Co@NPCC at 0.45 V *vs.* RHE in 0.1 M KOH.

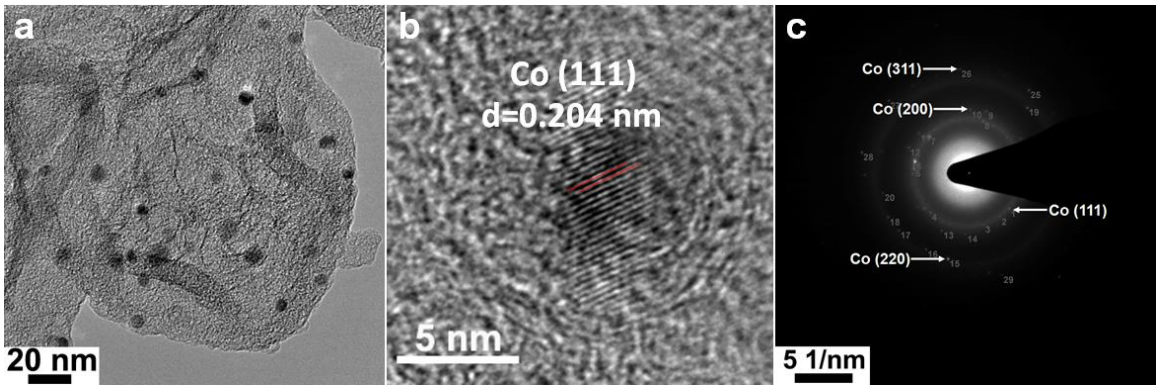

Fig. S18. TEM, HRTEM images and SAED pattern of Co@NPCC after accomplishing 10000 consecutive CV cycles in 0.1 M KOH.

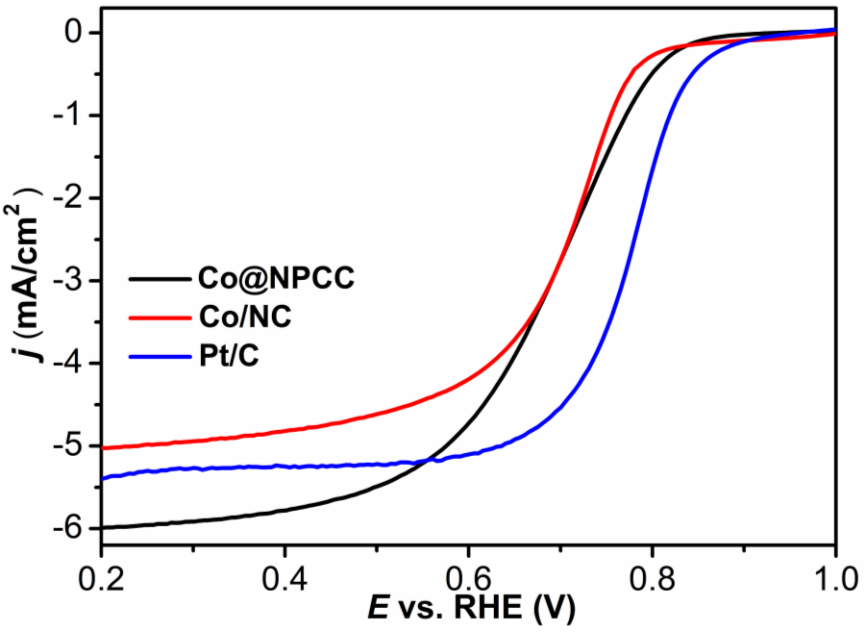

Fig. S19. ORR polarization curves for the various electrocatalysts at a rotation speed of 1600 rpm by RRDE technique in 0.05 M H_2SO_4.

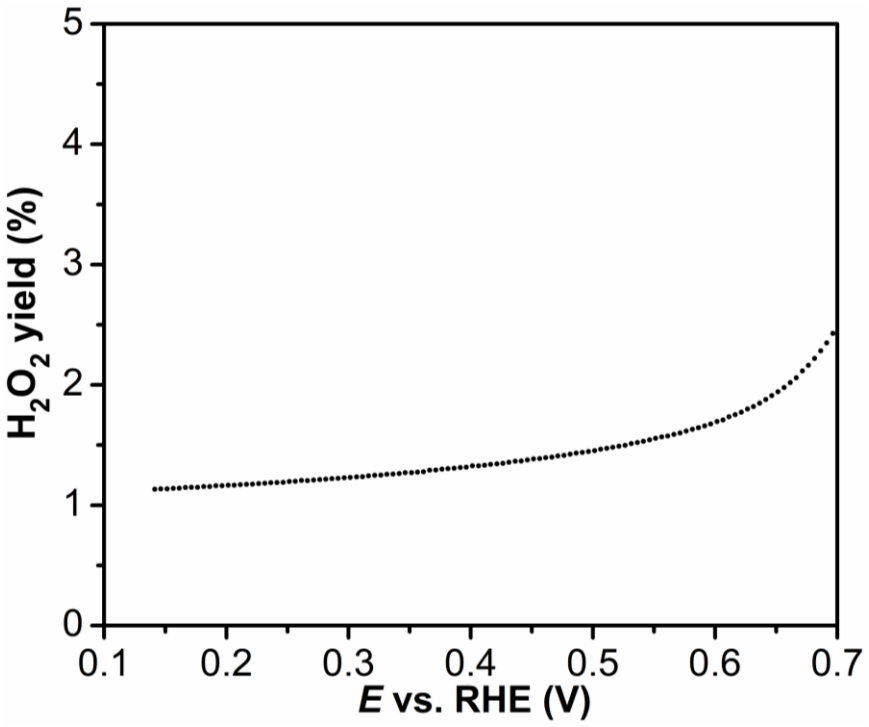

Fig. S20. H_2O_2 yield of Co@NPCC in 0.05 M H_2SO_4.

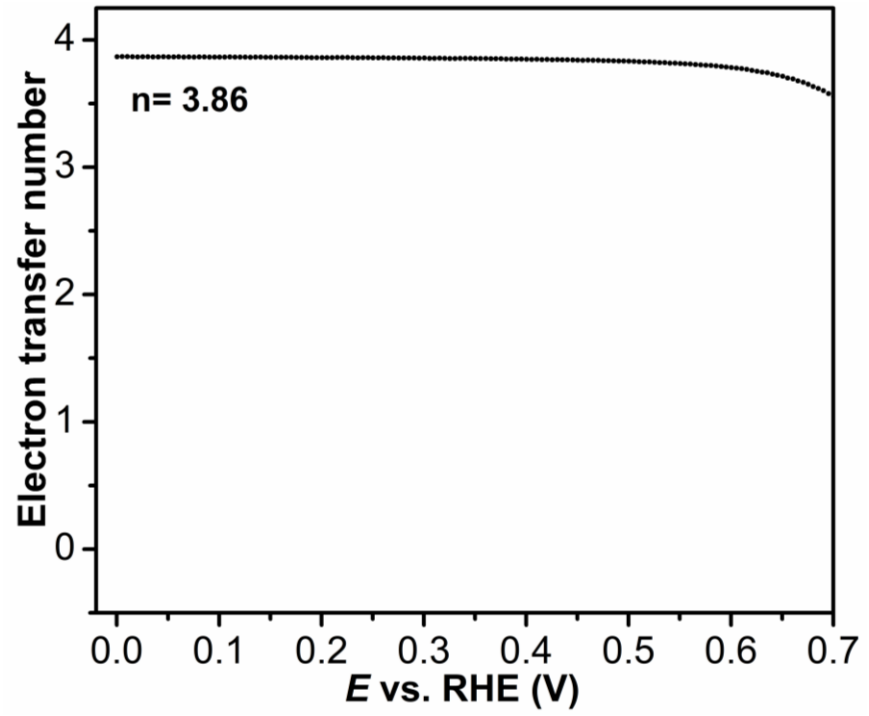

Fig. S21. electron-transfer number of Co@NPCC in 0.05 M H_2SO_4.

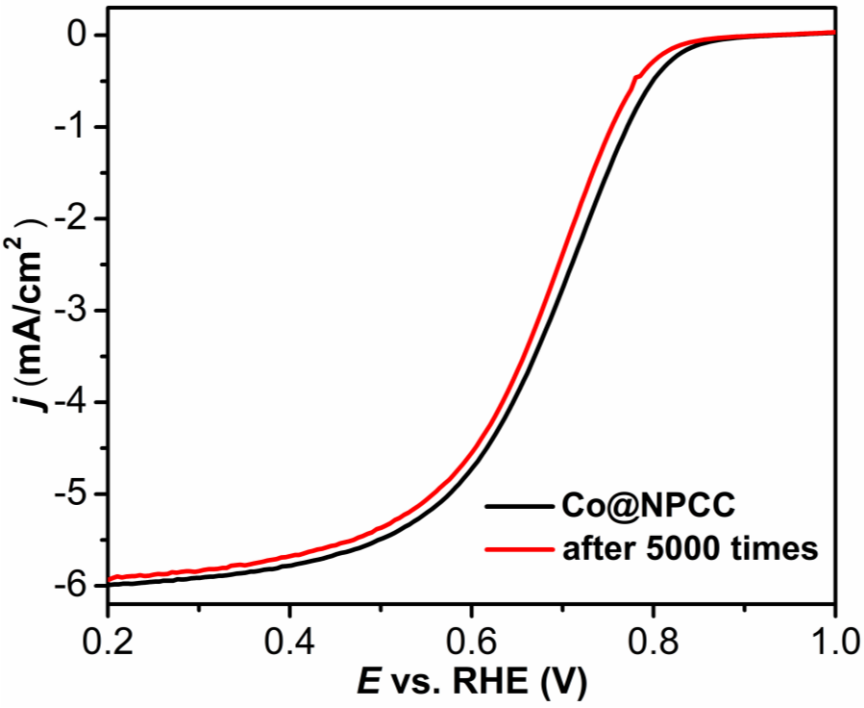

Fig. S22. LSV curves of Co@NPCC before and after 5000 cycles in O_2-saturated in 0.05 M H_2SO_4.

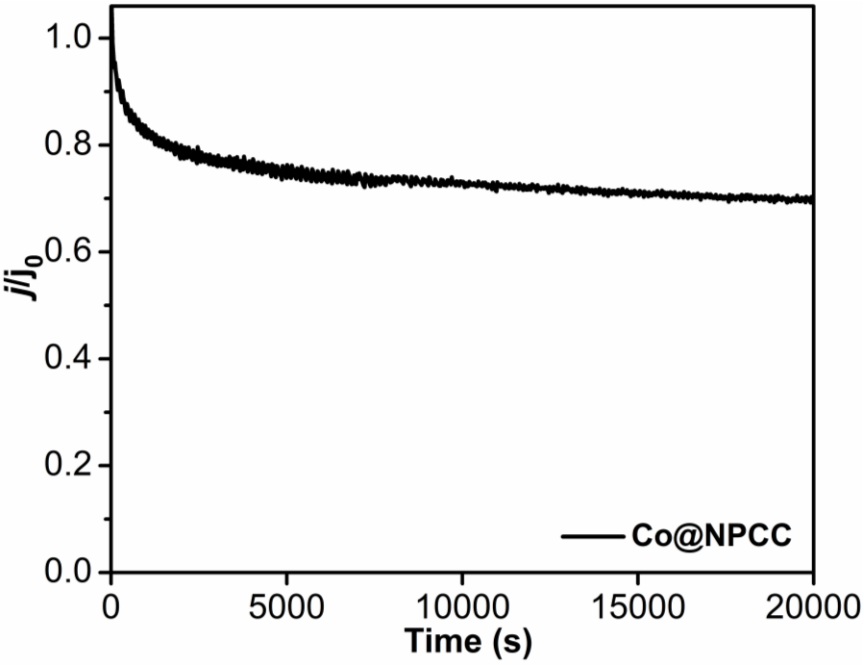

Fig. S23. The chronoamperometric test of Co@NPCC at 0.45 V *vs*. RHE in 0.05 M H_2SO_4.

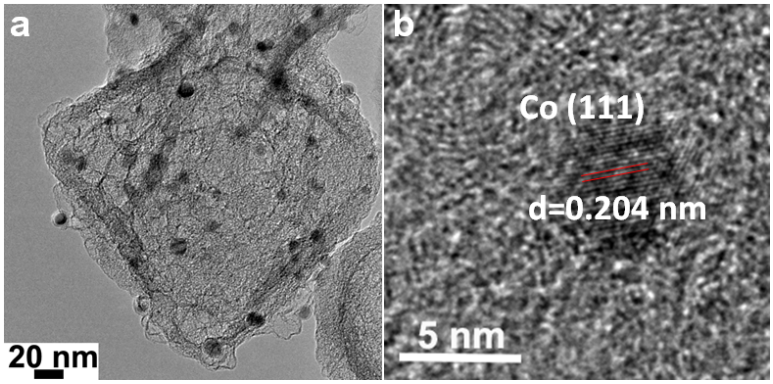

Fig. S24. TEM and HRTEM images of Co@NPCC after accomplishing 5000 consecutive CV cycles in 0.05 M H_2SO_4.

Table S1. ORR activities of the as−synthesized and reported materials in alkaline solution (electrode rotating speed is 1600 rpm, in 0.1 M KOH solution)

Catalyst	Loading mass (mg cm^{-2})	Onset potential (V)	Half−wave potential (V)	Current density (mA cm^{-2})	Ref.
Co@NPCC	0.1	1.02	0.9	5.2 (at 0.6 V)	this work
Co/NC	0.1	0.89	0.76	4.2 (at 0.6 V)	this work
Co@Co_3O_4@C–CM	0.1	0.93	0.81	~4.3 (at 0.6 V)	*Energy Environ. Sci.*, 2015, **8**, 568
Co@NC-3/1	0.1	1.15	0.93		*Adv. Energy Mater.* 2017, 1702048
Co@NPC-acid	0.2		0.75	5.3 (at 0.2 V)	*Dalton Trans.*, 2017, **46**, 15646
Fe−N/C−800	0.1	0.923	0.81	~ 6 (at 0.6 V)	*J. Am. Chem. Soc*., 2014, **136**, 11027
Fe–N–CNT–OPC	0.4	~0.96		~ 6 (at 0.5 V)	*Adv. Mater.*,2014, **26**, 6074
Fe−N−CNFs	0.6	0.93		5.12 (at 0.26V)	*Angew. Chem. Int. Ed*., 2015, **54**, 8179
Fe_X@NOMC	0.25	~0.9		~5.5 (at 0.5 V)	*Angew. Chem. Int. Ed.*, 2015, **54**, 1494
Fe_3C/NG−800	0.4	1.03	0.86	~ 6 (at 0.6 V)	*Adv. Mater*., 2015, **27**, 2521
PCN−FeCo/C	0.2	1.0	0.85	~ 5 (at 0.6 V)	*Adv. Mater., 2015*, **27**, 3431
PCNCo−20	0.1	0.92	0.84	~ 6 (at 0.6 V)	*Adv. Mater*. 2015, **27**, 5010
Fe−N−Carbon	0.0796	0.98		4.81 (at 0.45 V)	*J. Am. Chem. Soc*., 2015, **137**, 5555
Amaranthus derived carbon		1.135		4.38 (at 0.265 V)	*Energy Environ. Sci*., 2015, **8**, 221
Co−TA−800	0.3	0.95		4.2 at 0.60 V	*Angew. Chem. Int. Ed.*, 2016, **55**, 12470
FP−Fe−TA−N−850	0.3	0.98		5.0 (at 0.60 V)	*Angew. Chem. Int. Ed*., 2016, **55**, 1355
Co_3O_4/NPGC	0.2	0.97		5.84 (at 0.60 V)	*Angew. Chem. Int. Ed.*, 2016, **55**, 4977

NCNTFs	0.2	1.0		~ 5 (at 0.60 V)	*Nat. Energy*, 2016, **1**, 15006
N−Fe−CNT	0.2		0.87		*Nat. Comm.*, 2016, **4**, 1922
Co_3O_4/N−G	0.1	0.88	~0.83		*Nat. Mater.*, 2011, **10**, 780
Fe,N,S−codoped carbon	0.1		~0.81		*Adv. Mater*., 2013, **25**, 4794
S−Doped G			~0.73		*ACS Nano*, 2011, **6**, 205
B,N−doped CNTs			~0.75		A*ngew. Chem. Int. Ed.*,2011, **50**, 11756
N,S−codoped carbon	0.28		~0.82		*Adv. Mater*., 2013, **25**, 6284
CNT−G	0.485		~0.87		*Nat. Nanotech.* 2012, **7**, 394
N−doped G	0.051		~0.73		*ACS Nano*, 2013, **6**, 9541
SHG	0.2	1.01	0.87		*Adv. Mater*., 2017, **29**, 1604942
g−C_3N_4/carbon	0.085		~0.7		*Angew. Chem. Int. Ed.*, 2012, **51**, 3892
Fe_3C/C−800	0.6	1.05	0.83		*Angew. Chem. Int. Ed.*, 2016, **53**, 3675
NPC−Co45		0.9	0.79		*Nano Res.*, 2013, **6**, 293
Co@Co_3O_4/NC−1	0.21				*Angew. Chem. Int. Ed.*, 2016, **55**, 4087
h-Mn_3O_4-TMSLs		0.91	0.84	5.7 (at 0.2 V)	*J. Am. Chem. Soc.* 2017, **139**, 12133
TiCoN_x/N-rGO		0.982	0.902	~ 5.8 (at 0.60 V)	*J. Mater. Chem. A*, 2017, **5**, 5829
N-Co_9S_8/G	0.2	0.941		~6 (at 0 V)	*Energy Environ. Sci.*, 2016, **9**, 1320
MnS-NT@rGO		1 (1.0 M KOH)		1 (at 0.94 V)	*J. Power Sources*, 2017**, 362**, 1
Fe/NMC-11	0.51		0.862 (0.1 M NaOH)		*Adv. Energy Mater*. 2017, **7**, 1701154